

Measurements of optical absorption by chromophoric dissolved organic matter using a point-source integrating-cavity absorption meter

Rüdiger Röttgers and Roland Doerffer

Institute for Coastal Research, GKSS Research Centre Geesthacht, Max Planck Strasse 1, D-21502 Geesthacht, Germany

Abstract

The light absorption of 0.22- μm filtered seawater samples from the North Sea and the Atlantic Ocean was measured by a point-source integrating-cavity absorption meter (PSICAM), and the results were compared with measurement in a spectrophotometer. The absorption coefficient of this Gelbstoff or chromophoric dissolved organic matter (CDOM) ranges from high values of 0.103 to 0.519 m^{-1} at 442 nm for samples from the North Sea to very low values of 0.004 to 0.046 m^{-1} for samples from the Atlantic Ocean. At these low values, the influence of sample temperature and salinity on water absorption was significant. Hence, instrument-specific temperature and salinity coefficients were determined and, subsequently, used for correcting absorption data. Spectrophotometrically determined absorption was significantly higher at shorter wavelengths (< 442 nm) than absorption measured by the PSICAM, probably showing a significant influence of scattering by small particles remaining in the sample after filtration. At wavelengths between 442 and 500 nm, the correlation of PSICAM and spectrophotometer followed the 1:1 correspondence, whereas at longer wavelengths, the absorption was below the detection limit of the spectrophotometer. A similar agreement was obtained for the exponential slope of the CDOM absorption. The PSICAM matches the spectrophotometer results but is more sensitive and not affected by scattering. It will improve our ability to determine CDOM absorption in oligotrophic waters for the visible light spectral region.

The optical properties of dissolved organic matter (DOM) are one major inherent optical property of natural water. The colored compounds of the total DOM pool in water are called chromophoric dissolved organic matter (CDOM). For methodological reasons, it would be better called Gelbstoff (Kalle 1949, or yellow substances) because the sample is taken and simply filtered and, hence, includes all dissolved, colloidal, and particulate material that passes a specific filter (typically of 0.22 μm pore size). The determination of CDOM absorption is one key issue for optical measurements related, e.g., to optical remote sensing, to global or regional biogeochemistry of DOC (the carbonic part of DOM, Hansell and Carlson 2002), or simply for a reference measurement used to determine the particulate absorption.

The variability of CDOM absorption is large, ranging from very high values in rivers, with high loads of terrigenous mate-

rial, to medium values in coastal waters, which are highly influenced by riverine water inflow, and to very low values in remote, oligotrophic areas of the open ocean. The typical absorption spectrum of CDOM at the water surface is that of a curve exponentially decreasing with wavelength, showing higher absorption at shorter wavelengths of the ultraviolet and blue spectral regions (Bricaud et al. 1981). Absorption at longer wavelengths (>600 nm) is very low, and a significant absorption of CDOM at >700 nm is still under discussion, as it has not yet been measured accurately enough.

A method typically used to measure CDOM absorption is to determine its attenuation in a dual-beam spectrophotometer equipped with a glass or quartz-glass cuvette. When using a 10-cm cuvette in a dual-beam spectrophotometer, absorption values below 0.01 m^{-1} cannot be determined with a high accuracy. The use of a longer optical pathlength is one major contribution for improvements, but it is limited due to scattering losses in beam attenuation systems like spectrophotometers (Bricaud et al. 1981). The use of liquid waveguide systems with reflective walls allows performing CDOM measurements using pathlengths of several meters (D'Sa et al. 1999, Miller et al. 2000, 2002). Here, the influence of scattering is reduced but not totally prevented (e.g., losses by back-scattering). These systems were proven to be as accurate as spectrophotometers but more sensitive (D'Sa et al.

rroettgers@gkss.de

Acknowledgments

We thank the crews of RV *Polarstern*, RV *Südfall*, and MV *Wappen von Hamburg* for their help during the different cruises. Kerstin Heymann, Hajo Krasemann, and Wolfgang Schönfeld conducted some of the photometric CDOM determination and helped during the *Wappen of Hamburg* cruises to Helgoland. Henning Wehde and Martina Gehrung collected samples from the ferry between Harwich and Cuxhaven.

1999, Miller et al. 2002), and they have the advantage of using relatively small sample volumes. As an alternative, an integrating-cavity absorption meter (ICAM), combines a relatively larger mean optical pathlength with the reduction of adverse scattering effects to insignificant levels, but, so far, it has rarely been used with natural water samples (e.g., Pope et al. 2000). We constructed a simple ICAM type, a so-called point-source integrating-cavity absorption meter (PSICAM, Kirk 1997) and evaluated its performance by using solutions of a humic acid sodium salt and CuSO_4 (Röttgers et al. 2005). The PSICAM consists of a spherical cavity made out of a white, highly reflective plastic material and a central scattering sphere as the light source. The reflectivity of the inner wall of the spherical cavity is the most sensitive parameter for the determination of the absorption coefficient and has to be determined exactly (Leathers et al. 2000) for calibrating the instrument.

The need to calibrate the PSICAM makes it necessary to conduct comparisons with a spectrophotometer to evaluate the accuracy of the PSICAM. The PSICAM measurements showed a good correlation with the photometric results, with at least the same accuracy but a higher sensitivity than a spectrophotometer system. Differences were found at very low absorption values, near the sensitivity limits of the photometer (10 cm cuvette). This article now reports on a comparison made with a large set of natural water samples taken at different geographical positions in the North Sea, through the Atlantic Ocean, and at different times of the year.

Materials and procedures

Sampling—Water samples from mainly the surface but also from up to 200 m were taken at different occasions during the year 2005: by an automatic sampler onboard a ferry between Cuxhaven (Germany) and Harwich (England), manually onboard a ferry between Cuxhaven and the island of Helgoland, manually onboard of RV *Südfall* on two cruises between Büsum (Germany) and Helgoland, and manually onboard RV *Polarstern* during the cruise ANTXXIII/1 from Bremerhaven (Germany) to Cape Town (South Africa). The salinity and temperature for each sample were recorded for a later salinity correction. The samples were filtered first through a glass-fiber filter (GF/F, Whatman), and then through a sample-rinsed 0.22 μm membrane filter (Millipore GSWP) following the procedures described in Tilstone et al. (2002). The samples were either measured directly after filtration in case of the PSICAM or stored and measured in the lab less than 48 h later, normally at the next day. The absorption spectrum of each sample was used to determine the exponential slope s . This was done by fitting the data between 350 and 500 nm to an exponential function as

$$a_{\text{cdom}}(\lambda) = a_{\text{cdom}}(442\text{nm}) \times e^{-s(\lambda - 442)} \quad (1)$$

where λ is the wavelength, and $a_{\text{cdom}}(\lambda)$ the absorption coefficient at wavelength (λ). The wavelength 442 nm is used as reference wavelength because it is a common band in ocean color sensors.

CDOM absorption determination with a spectrophotometer—Measurements of CDOM absorption are done in accordance with Tilstone et al. (2002) in a LAMBDA 800 UV/VIS dual-beam spectrophotometer (Perkin Elmer). Fresh or stored samples are kept in the lab at room temperature for 2 to 6 h before measuring. The temperature of the samples and the reference (purified water) is controlled with an electronic thermometer. Temperature differences were always $< 0.2^\circ\text{C}$. The photometer is turned on and set up 30 min before the first measurement. Scans are taken from at least 750 to 350 nm, with a speed of 150 nm min^{-1} , and a slit width of 2 nm. All glass windows of the photometer and the cuvette are checked visually and, if necessary, cleaned first with high-performance liquid chromatography (HPLC)-grade ethanol and then with purified water. The baseline is recorded with the acid-cleaned 10 cm quartz-glass cuvette filled with purified water (Elix, Milli-Q plus TOC reduction, Millipore) and an empty reference beam. The purified water is checked for scattering particles by filtration through a 0.22 μm filter holder (SPARTAN A 25 mm) using a new 50 mL plastic syringe. The filter holder and the syringe are cleaned beforehand by filtering and discarding 3 times 50 mL purified water. Sample contamination by the filter holder and the syringe after this cleaning could not be observed. Absorbance of this filtered, purified water is determined; if necessary (absorbance < -0.0005 optical density [OD]), fresh filtered purified water is taken as reference. Each sample is measured at least two times by filling and cleaning the cuvette a second time, to check repeatability.

Because it was observed that the sample had a higher attenuation after storage overnight (see below), each sample is filtered a second time, just before measuring, into a 100 mL acid-cleaned small-necked quartz-glass bottle using the already cleaned 0.22 μm filter holder and syringe. The first filtered 30 mL of the sample are used to rinse the filter holder, the syringe, and the bottle three times, before 40 mL are filtered into the bottle. Filtration into an extra bottle before pouring the sample into the cuvette removes any air bubbles build after filtration. It is made sure that this handling does not change the sample temperature by checking the temperature after the filtration process. This procedure mostly reduces the absorption and increases the repeatability (e.g., see Blough et al. 1993). The measured attenuation is taken as absorption, A , where $A = -\log_{10}T$, and T is the transmission. The absorption coefficient, a , is calculated by $a = 2.303A/L$, where L is the pathlength of the cuvette in meters, and the factor 2.303 converts \log_{10} to \log_e . The absorption coefficient is corrected for the difference in salinity between sample and reference using the obtained salinity coefficient, Ψ_s (see below).

Quality control is performed before each scan by observing the absorption value at 750 nm. CDOM solutions with salinity 0 and with negligible temperature difference to the reference ($< 0.2^\circ\text{C}$) should have OD around the peak to peak noise of the spectroradiometer (0.0005). In case the salinity is higher, minimum OD at 750 nm can increase to +0.002 due to

the salinity influence on the water absorption. If OD at 750 nm differs from the minimum value for each specific salinity, the cuvette is taken out of the spectrophotometer and checked again. In most cases, the OD is too high implying additional attenuation due to bubbles, a dirty surface, or dust particles. Removing newly built bubbles or cleaning the cuvette windows with ethanol and afterward with purified water generally reduces the OD to the expected values. If not, the sample aliquot is discarded and a new aliquot taken. Occasionally, the spectra showed artificial attenuation peaks due to a dust particle crossing the light beam while scanning, or new bubbles were built during scanning. In both cases the measurement was repeated with a new sample aliquot. Regularly, the baseline is controlled by measuring purified water in between measurements of samples. Occasionally, the baseline changes slightly due to a shift in the room temperature and, hence, a difference in temperature of the actual sample and that of the beforehand measured reference; in such a case the baseline is recorded again.

CDOM absorption determination with the PSICAM—The 0.22-filtered sample water is measured as soon as possible with the PSICAM system as described in Röttgers et al. (2005). Therefore the cavity of the PSICAM is filled with purified water, air bubbles are removed from the cavity wall and the central light sphere by gentle shaking, and the reference intensity spectrum is recorded between 350 and 726 nm (or up to 800 nm, dependent on the detector type). Afterwards, the filtered sample water is poured into the cavity in the same way, and the sample intensity spectrum is recorded. The cavity is rinsed and filled with purified water again, and a second reference intensity spectrum is recorded. The two reference spectra are used to calculate two “transmissions” (sample/reference) and, further, two absorption coefficient spectra. The mean of these two spectra is taken as the real absorption coefficient spectrum. This procedure corrects for small but constant intensity shifts in the PSICAM induced by unstable light focusing onto the fiber-optic connection. Each sample is measured at least two times in this way to control repeatability. The overall precision was high (see below) and repetitions for a single sample would not be necessary for high Gelbstoff concentrations.

The necessary calibration of the PSICAM consists of regular determinations of the total cavity reflectivity spectrum, which is the most critical factor for the absorption determination with a PSICAM (Leathers et al. 2000). This is done as described in Röttgers et al. (2005) by using solutions of the dye nigrosine (Certistain®, Merck) with maximum absorption between 1 and 3 m⁻¹. The absorption of the nigrosine solution is determined spectrophotometrically as described above for Gelbstoff and used to determine the reflectivity spectrum of the PSICAM cavity by conducting a single measurement against purified water. After each reflectivity determination and otherwise once a day, the PSICAM is cleaned using a NaOCl bleach (Riedel de Haën, 500 µL NaOCl solution in 500 mL water). The bleach is filled in the PSICAM cavity for 30 min and, afterward, the

cavity is rinsed a few times with purified water. In addition, once a day, the PSICAM is disassembled and the inner surface cleaned with HPLC-grade ethanol.

Additional errors could arise from Raman scattering and CDOM fluorescence. As pure water serves as the reference, Raman scattering by water is the same for reference and sample. The influence of Raman scattering of water and CDOM fluorescence was not observed to be significant for the PSICAM measurements (Röttgers et al. 2005).

Assessment

Determination of salinity and temperature coefficients for water absorption—The effect of salinity on pure water absorption for measurements with the photometer and the PSICAM was determined to obtain instrument-specific salinity correction coefficients, Ψ_s^i . It is assumed that the salinity effects are partly due to real changes of the water absorption and partly due to a change of the refractive index with salinity (see Sullivan et al. 2006). The effect of the refractive index is instrument-specific, but should be negligible for the PSICAM, because of the larger volume examined. Therefore, we determined Ψ_s^i separately for the PSICAM and the spectrophotometer setup. The two different salinity coefficients were determined by measuring the attenuation of different NaCl solutions against purified water. It is assumed that the influence of NaCl on absorption is the same as that of salt in natural oceanic waters, as Na⁺ and Cl⁻ ions constitute 86% of all ion species in seawater. For this kind of determination, Sullivan et al. (2006) showed that on a mass basis NaCl is a good proxy for the other ions in seawater. Different amounts of 99.9% pure NaCl (pro analysis grade, Merck) were diluted in 1000 mL purified water to gain 5 different solutions with concentrations between 5 and 90 g kg⁻¹. Beforehand, the solid NaCl was heated to 450°C for 4 h to remove any organic material contaminating the salt. The actual salinity was controlled with an electronic conductivity meter (WTW, Germany) after the solutions were filtered through 0.22 µm membrane filter (GSWP, Millipore). The absorption change of each of these solutions was determined with the PSICAM using purified water without NaCl as a reference. During these measurements, the temperature was controlled and temperature differences were less than ±0.2°C. Some measurements were conducted at different temperatures to check whether temperature influences Ψ_s^i . This was not observed. The absorption change showed a linear relationship with salinity and a linear regression through the absorption at different salinities was used to gain a salinity correction coefficient at each wavelength. The measurement of Ψ_s^i for the photometer was done by simply determining the attenuation of a 90 g kg⁻¹ solution five times and dividing the mean attenuation by the mass concentration (90 g kg⁻¹) to get the specific coefficient, i.e., per salinity (m⁻¹ S⁻¹).

A typical CDOM measurement with a spectrophotometer shows a large trough at about 732 nm and positive values at

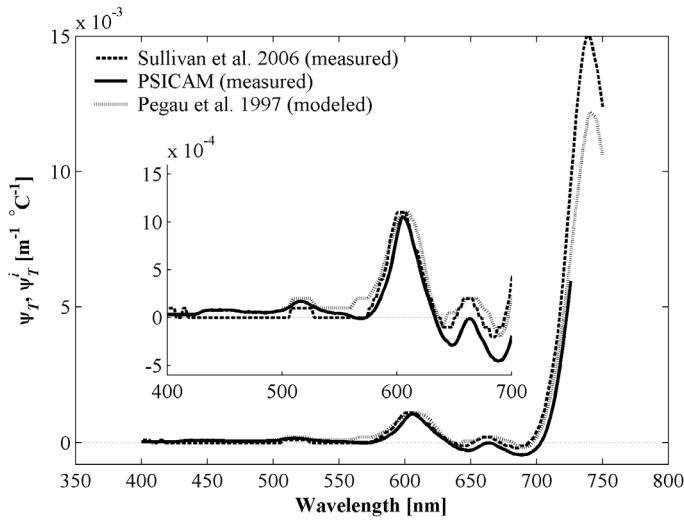


Fig. 1. Temperature dependency of pure water absorption, Ψ_T , as a function of wavelength. Shown is the instrument-specific coefficient, Ψ_T^i , for the PSICAM together with published data of Ψ_T (see legend). The inset shows the same data on a different scale to emphasize the small peaks at ~ 440 and ~ 510 nm.

wavelengths > 740 nm. These artifacts are quite often ignored or related to differences in temperature or the refractive index (Green and Blough 1994). Furthermore, this effect is seen as a constant offset and the absorption spectrum is “corrected” by subtracting a mean value of the absorption between, e.g., 700 and 750 nm, from the absorption at all wavelengths (e.g., Green and Blough 1994, D’Sa et al. 1999). However, the influence of temperature takes place at different wavelengths, showing peak at ~ 606 , ~ 662 , and ~ 742 nm (see Fig. 1), and the small temperature difference of less than $\pm 0.2^\circ\text{C}$ are not sufficient for inducing a trough like that at 732 nm.

The previously published data for the salinity coefficient for pure water absorption, Ψ_S , (see Pegau et al. 1997, and references therein), were not sufficient regarding wavelength resolution and accuracy to explain these absorption peaks induced by salinity difference. The first hyperspectral spectra of Ψ_S were determined recently with a PSICAM prototype (Brando et al. 2004) and an AC-S instrument (Wetlabs; Sullivan et al. 2006, Fig. 2) and showed clear peaks at ~ 620 , ~ 710 , and > 735 nm. However, these spectra cannot explain the large trough at 732 nm for the spectrophotometric determination.

As for the data of Sullivan et al. (2006), the influence on absorption was linearly related to the salinity, and no interference between temperature and salinity on the water absorption could be observed (data not shown). Fig. 2 shows Ψ_S^i determined for the PSICAM and the spectrophotometer setup together with Ψ_S determined by Sullivan et al. (2006). All three spectra show some similarities (e.g., peaks at ~ 620 and ~ 666 nm) but also some differences in the absolute values over the whole spectrum. A large trough at 732 nm is observed for the spectrophotometer setup but is not visible in the other

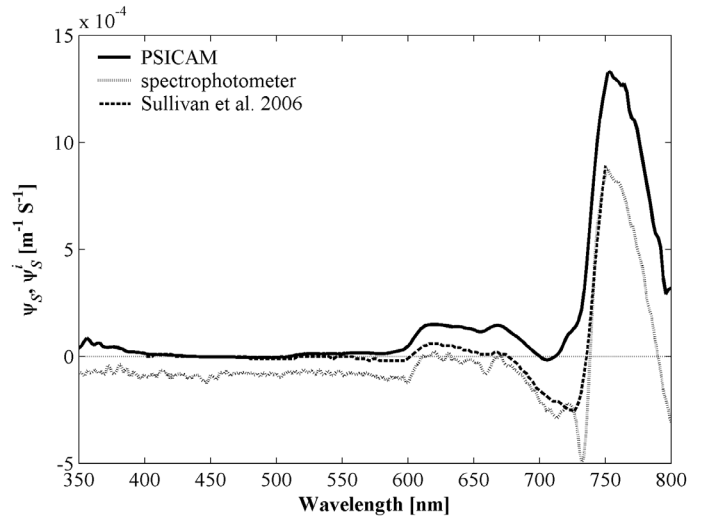


Fig. 2. Salinity dependency of pure water absorption, Ψ_S , as a function of wavelength. Shown are the instrument-specific coefficients, Ψ_S^i , for the PSICAM and the spectrophotometer together with published data for Ψ_S of Sullivan et al. (2006).

spectra. This trough can explain the artifact at 732 nm for the spectrophotometric absorption determination. Values of Ψ_S^i of the spectrophotometer setup are lower over all wavelengths when compared to Ψ_S^i of the PSICAM or the Ψ_S data of Sullivan et al. (2006). This might be due to the molecular scattering of the salt ions or the influence of the change in refractive index with salinity. Sullivan et al. (2006) observed a similar offset for the attenuation channel of the AC-S instrument when compared with the absorption channel. As this effect is linearly related to salinity at all wavelengths, we did not perform further corrections for this negative offset. The increase of the coefficient in both Ψ_S^i -spectra at < 400 nm is attributed to impurities in the NaCl solution, which can contain traces of CDOM remaining after insufficient combustion, because we did not use optical grade NaCl as done by Sullivan et al. (2006). Hence, for the PSICAM, the salinity correction coefficient was set to zero at wavelengths < 400 nm.

The temperature correction coefficient, Ψ_T^i , for the PSICAM was determined by measuring water of 25°C against water of 10°C . A mean Ψ_T^i was calculated by dividing the averaged ($n = 5$) spectra of the change in absorption by the temperature difference (15°C). Figure 1 shows Ψ_T^i , and some published temperature coefficient of water absorption Ψ_T . Ψ_T^i is similar to the modeled Ψ_T of Pegau et al. (1997) and the measured one of Sullivan et al. (2006) and that of Langford et al. (2001) (data not shown). But it shows some deviations at wavelengths < 500 nm and > 600 nm, which are probably related to instrument-specific optical changes with a shift in temperature. The relative effect on absorption of the slightly positive values of Ψ_T^i at wavelengths < 500 nm is negligible due to a relatively high absorption, i.e., the typical exponential increase with shorter wavelengths of a_{CDOM} . Ψ_T^i was used to correct for

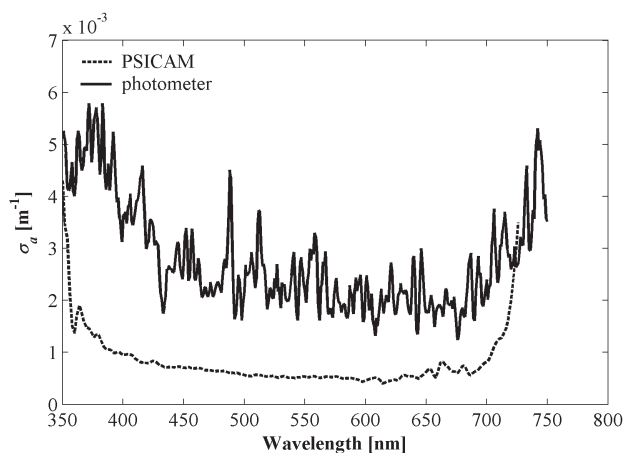


Fig. 3. Precision as a function of wavelength for absorption measurements with the PSICAM and the photometer. Each precision is shown as the averaged standard deviation, σ_a , of the absorption coefficient a determined for several measurements with different solutions of a humic acid sodium salt. Each single standard deviation was determined by repetitive measurements of the same humic acid solution ($n = 10$).

temperature deviations between sample and reference, a small error remains due to the error in the determination of Ψ_r^i and the error of the temperature determination, which was at least $\pm 0.2^\circ\text{C}$.

Determination of the precision for photometric and PSICAM measurements—To determine the precision (standard deviation) of the two absorption methods applied, we measured (10 times for each) the absorption coefficient spectrum for pure water and for a humic acid solution ($a_{442\text{nm}} \sim 0.02$ for PSICAM, and $a_{442\text{nm}} \sim 0.07 \text{ m}^{-1}$ for the spectrophotometer) both against pure water as the reference. The solutions were made by diluting small amounts of humic acid sodium salt (Sigma-Aldrich) in purified water using acid-cleaned 1 L glass bottles (Duran, Schott). Each solution was filtered through a $0.22 \mu\text{m}$ membrane filter (GSWP, Millipore) shortly before measuring. The photometric measurement was done as described above by using new aliquots for each of the 10 repetitive measurements. For the PSICAM system, the sample was filled in the cavity 10 times and the spectrum determined, alternating with rinsing and filling the cavity with purified water and the determination of the reference spectrum (see above). The mean and standard deviation of these 10 measurements were calculated, and the standard deviations determined for the two separate determinations (pure water and humic acid solution) were averaged (Fig. 3).

The precision of the spectrophotometer is only slightly wavelength-dependent with a mean value of $\pm 0.0028 \text{ m}^{-1}$ and minimum values of ca. 0.0022 m^{-1} . The precision for the PSICAM shows a higher wavelength-dependence, with higher standard deviations at shorter ($< 400 \text{ nm}$) and longer ($> 700 \text{ nm}$) wavelengths where the light intensities inside the PSICAM are already low. The mean precision of the PSICAM determination is about $\pm 0.0008 \text{ m}^{-1}$ and the minimum values are about

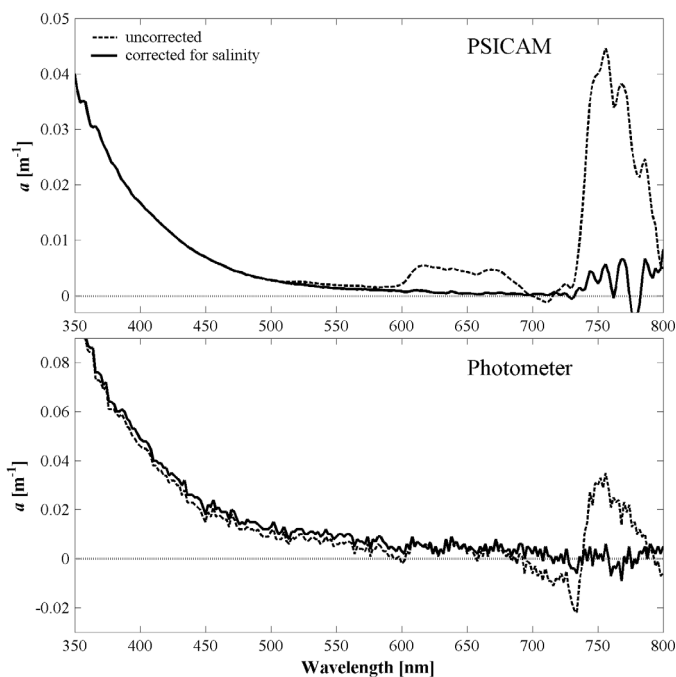


Fig. 4. Absorption spectra corrected for salinity effects using the instrument-specific salinity coefficient, Ψ_s^i . Shown is one example for PSICAM and one for spectrophotometric data. Depicted are the original spectra (dotted lines) and the absorption spectra after a salinity correction is applied (solid lines).

$\pm 0.0005 \text{ m}^{-1}$. The precision of the PSICAM determination is, hence, about four times better than that of the spectrophotometric determination.

The overall accuracy of the spectrophotometric method is estimated using the technical description of the photometer, i.e., $\pm 0.05\%$ for transmission. When using a 10-cm cuvette, this accuracy for the absorption coefficient would be $\pm 0.005 \text{ m}^{-1}$. However, the accuracy of our gray-glass standard for photometer calibration is ± 0.006 for an absorbance value of ca. 0.3, hence, the uncertainty of the photometer cannot be given better than $\pm 2\%$ at higher absorption values. Values below 0.1 m^{-1} would have relative errors of $\pm 5\%$ and higher due to the instrument accuracy of 0.005 m^{-1} . As the PSICAM is calibrated using spectrophotometric measurements of solution with relatively high absorption values, the accuracy of the PSICAM cannot be better than $\pm 2\%$. But this 2% error is valid for absorption values $< 0.1 \text{ m}^{-1}$ as well. Errors in the corrections for salinity and temperature will influence accuracy at wavelengths $> 500 \text{ nm}$.

Comparison of PSICAM and spectrophotometer—The two instrument-specific salinity-coefficient spectra are subsequently used to correct the obtained absorption spectra. Figure 4 shows exemplary results of this correction for a PSICAM and a photometric measurement of a sample from the Atlantic Ocean.

The standard deviation for the PSICAM- Ψ_s^i spectrum (data not shown) showed some large variation at wavelengths above

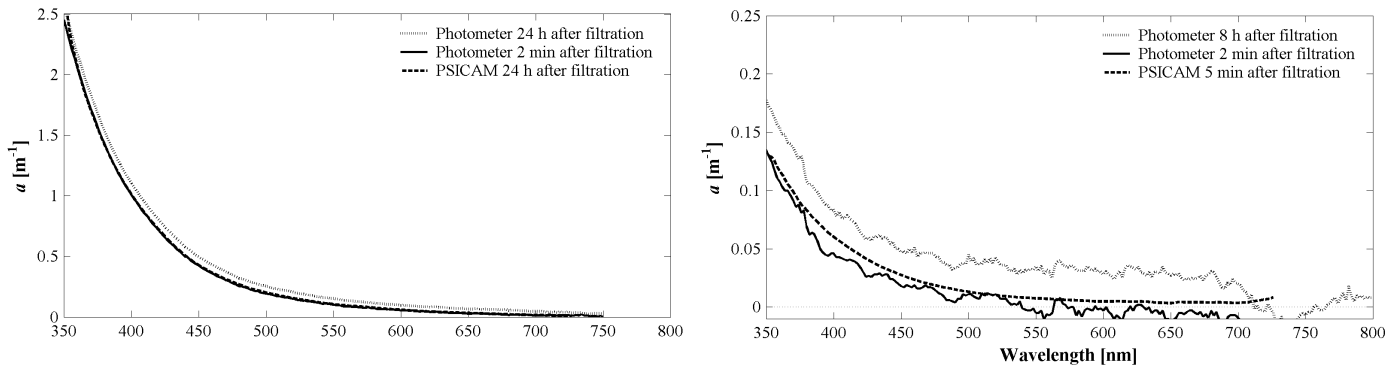


Fig. 5. Absorption coefficient as a function of wavelength determined with the PSICAM and with the spectrophotometer. Shown are different measurements of the same sample performed at a specific time after filtration through a $0.22 \mu\text{m}$ filter. The left panel shows an example from the North Sea with high absorption, the right one a sample from the Atlantic Ocean with low absorption. Note the different scale of the y-axis. The two curves of “photometer 2 min after filtration” and “PSICAM 24 h after filtration” are on top of each other.

700 nm that will induce a relative large error in absorption at these wavelengths after the salinity correction (see Fig. 4). This higher variability is also visible in a lower precision at these wavelengths (see Fig. 3). We suppose that this is due to small changes in temperature or in the optical setup. Manipulating the different optically active parts as done during a regular measurement could induce small changes in the optical setup. This higher variability is the reason why PSICAM measurements are yet not reliable at wavelengths > 730 nm. A

second reason is the instability of the light intensity inside the PSICAM, whose influence is largest at low CDOM absorption and at high water absorption. The following data comparison will be focused on wavelengths between 360 and 700 nm.

Part of the samples were taken during short transects from Cuxhaven to the island of Helgoland. The samples were filtered a few hours later, but CDOM absorption could only be measured the next day. It was observed that an additional filtration through a $0.22 \mu\text{m}$ filter shortly before the measurement

Table 1. Optical absorption parameter s , $a_{370\text{nm}}$ and $a_{442\text{nm}}$ of CDOM samples from the North Sea

Station nr	Position North Sea	Photometer			PSICAM		
		s (nm^{-1})	$a_{370\text{nm}}$ (m^{-1})	$a_{442\text{nm}}$ (m^{-1})	s (nm^{-1})	$a_{370\text{nm}}$ (m^{-1})	$a_{442\text{nm}}$ (m^{-1})
F0110	53° 51.01' N 6° 59.83' E	0.0176	0.791	0.222	0.0177	0.787	0.224
F0109	53° 44.52' N 6° 14.83' E	0.0170	0.499	0.148	0.0171	0.481	0.142
F0106	53° 4.10' N 3° 59.83' E	0.0159	0.361	0.115	0.0166	0.349	0.107
F0203	52° 16.84' N 2° 11.93' E	0.0187	0.338	0.088	0.0171	0.352	0.103
F0202	52° 0.33' N 1° 35.82' E	0.0174	0.441	0.126	0.0171	0.441	0.130
C1802	54° 7.09' N 8° 19.60' E	0.0179	1.586	0.435	0.0179	1.570	0.444
C1803	54° 8.41' N 8° 8.76' E	0.0174	1.083	0.308	0.0177	1.098	0.316
C1804	54° 9.54' N 7° 57.42' E	0.0174	0.626	0.179	0.0176	0.595	0.169
C1901	54° 9.30' N 7° 57.66' E	0.0175	0.635	0.181	0.0177	0.626	0.179
C1902	54° 8.46' N 8° 5.41' E	0.0172	1.147	0.333	0.0180	1.106	0.311
C1903	54° 7.45' N 8° 14.46' E	0.0178	1.525	0.423	0.0182	1.477	0.411
C1904	54° 6.65' N 8° 22.15' E	0.0180	1.463	0.400	0.0181	1.343	0.374
C2101	53° 59.46' N 8° 25.40' E	0.0179	1.862	0.517	0.0178	1.808	0.519
C2102	54° 0.50' N 8° 18.72' E	0.0176	1.491	0.422	0.0180	1.502	0.424
C2103	54° 3.38' N 8° 9.26' E	0.0175	1.433	0.408	0.0181	1.412	0.394
C2105	54° 6.17' N 8° 2.30' E	0.0177	1.372	0.386	0.0178	1.363	0.388
C2201	53° 59.12' N 8° 33.42' E	0.0174	1.720	0.493	0.0177	1.703	0.490
C2202	53° 59.75' N 8° 23.20' E	0.0178	1.696	0.471	0.0177	1.656	0.474
C2203	54° 0.92' N 8° 16.38' E	0.0173	1.559	0.451	0.0174	1.495	0.434
C2204	54° 2.96' N 8° 9.52' E	0.0175	1.466	0.418	0.0176	1.418	0.409
C2205	54° 5.82' N 8° 2.96' E	0.0178	1.663	0.465	0.0177	1.580	0.452

All samples are taken from the surface.

Table 2. Optical absorption parameter s , a_{370nm} and a_{442nm} of CDOM samples from the Atlantic Ocean

Station nr	Position Atlantic Ocean	Photometer			PSICAM		
		s (nm^{-1})	a_{370nm} (m^{-1})	a_{442nm} (m^{-1})	s (nm^{-1})	a_{370nm} (m^{-1})	a_{442nm} (m^{-1})
P0102	46° 49.07' N 5° 18.15' W	0.0153	0.144	0.048	0.0153	0.118	0.039
P0104	45° 51.79' N 6° 37.43' W	0.0160	0.104	0.032	0.0159	0.091	0.029
P0105	46° 13.01' N 4° 5.67' W	0.0172	0.109	0.030	0.0159	0.099	0.031
P0106	45° 45.02' N 5° 31.48' W	0.0135	0.093	0.033	0.0167	0.063	0.019
P0108	33° 33.73' N 14° 30.36' W	0.0188	0.047	0.012	0.0173	0.032	0.009
P0109	29° 35.97' N 16° 19.15' W	0.0180	0.045	0.012	0.0209	0.021	0.004
P0110	25° 31.83' N 17° 51.67' W	0.0217	0.029	0.006	0.0183	0.029	0.008
P0111	22° 30.01' N 20° 30.18' W	0.0196	0.056	0.014	0.0172	0.051	0.015
P0112	18° 22.44' N 20° 55.65' W	0.0201	0.076	0.018	0.0174	0.067	0.019
P0114	10° 36.97' N 20° 8.13' W	0.0227	0.040	0.007	0.0149	0.027	0.009
P0115	7° 1.38' N 17° 29.27' W	0.0168	0.027	0.009	0.0184	0.022	0.006
P0116	3° 41.83' N 14° 43.00' W	0.0188	0.029	0.008	0.0187	0.024	0.006
P0117	0° 16.11' N 12° 0.75' W	0.0196	0.048	0.011	0.0174	0.032	0.009
P0118	0° 41.73' S 11° 15.89' W	0.0169	0.049	0.015	0.0147	0.042	0.014
P0119	2° 9.37' S 10° 8.07' W	0.0101	0.066	0.032	0.0154	0.040	0.013
P0120	8° 47.75' S 4° 58.70' W	0.0223	0.064	0.012	0.0174	0.049	0.014
P0121	11° 52.00' S 2° 30.78' W	0.0251	0.048	0.008	0.0169	0.035	0.010
P0122	14° 15.99' S 0° 35.77' W	0.0236	0.043	0.008	0.0161	0.038	0.012
P0123	17° 51.99' S 2° 19.25' E	0.0166	0.054	0.017	0.0158	0.043	0.014
P0124	21° 6.34' S 4° 59.70' E	0.0196	0.042	0.010	0.0173	0.033	0.009
P0125	24° 31.59' S 7° 52.64' E	0.0169	0.049	0.015	0.0147	0.043	0.015
P0127	25° 57.76' S 9° 21.85' E	0.0164	0.044	0.014	0.0147	0.036	0.012
P0214	34° 12.04' N 14° 6.45' W	0.0308	0.055	0.005	0.0178	0.033	0.009
P0215	32° 23.00' N 15° 13.29' W	0.0184	0.061	0.015	0.0206	0.029	0.006
P0216	30° 16.07' N 16° 29.34' W	0.0199	0.056	0.012	0.0189	0.040	0.010
P0217	26° 9.400' N 17° 9.799' W	0.0225	0.046	0.009	0.0207	0.029	0.006
P0219	21° 31.09' N 20° 51.58' W	0.0162	0.071	0.022	0.0173	0.054	0.016
P0221	17° 26.31' N 20° 56.68' W	0.0203	0.050	0.012	0.0185	0.039	0.010
P0222	14° 37.54' N 20° 58.39' W	0.0233	0.044	0.008	0.0158	0.037	0.011
P0223	12° 32.78' N 20° 32.02' W	0.0250	0.040	0.006	0.0210	0.030	0.006
P0224	9° 23.73' N 19° 29.38' W	0.0161	0.044	0.014	0.0214	0.028	0.006
P0225	7° 34.82' N 17° 57.85' W	0.0178	0.045	0.012	0.0204	0.031	0.007
P0226	6° 8.57' N 16° 45.62' W	0.0251	0.029	0.005	0.0212	0.025	0.005
P0227	4° 17.77' N 15° 13.13' W	0.0234	0.034	0.006	0.0194	0.025	0.006
P0228	2° 35.13' N 13° 48.97' W	n.d.	0.030	0.001	0.0215	0.024	0.005
P0229	0° 46.08' N 12° 24.16' W	0.0207	0.044	0.010	0.0187	0.037	0.010
P0231	3° 11.54' S 9° 19.31' W	n.d.	0.039	-0.005	0.0169	0.036	0.010
P0232	4° 48.77' S 8° 3.53' W	0.0186	0.046	0.013	0.0173	0.040	0.011
P0233	8° 21.37' S 5° 17.08' W	0.0212	0.076	0.016	0.0176	0.061	0.017
P0234	9° 46.08' S 4° 10.38' W	0.0248	0.056	0.009	0.0188	0.045	0.011
P0235	13° 48.07' S 0° 58.16' W	0.0274	0.045	0.006	0.0160	0.037	0.011
P0236	15° 25.54' S 0° 20.19' E	0.0233	0.050	0.009	0.0162	0.039	0.012
P0238	18° 48.86' S 3° 5.62' E	0.0207	0.038	0.009	0.0160	0.040	0.012
P0239	20° 34.20' S 4° 32.64' E	0.0188	0.051	0.013	0.0167	0.034	0.010
P0240	22° 10.11' S 5° 52.71' E	0.0162	0.068	0.021	0.0166	0.054	0.016
P0241	23° 58.24' S 7° 24.10' E	0.0188	0.054	0.014	0.0157	0.043	0.014

All samples are taken from the surface. Samples from greater depth are not shown. n.d., not determined.

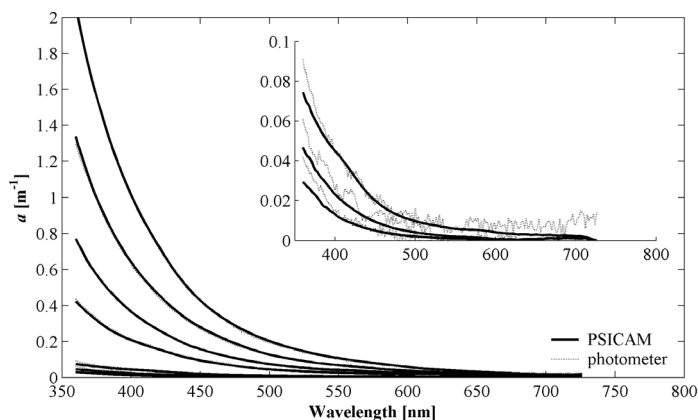


Fig. 6. Typical examples of absorption measured for the same sample with the PSICAM and with the spectrophotometer. Shown are the results of seven different samples with absorption at 400 nm between 0.01 and 1 m^{-1} . The inset shows the three samples with the lowest absorption on a different scale.

reduces the absorption (better called attenuation in this case) determined spectrophotometrically, especially at longer wavelengths, but did not influence the absorption determined with the PSICAM. A few samples were kept for another 8 or 24 h, and the measurements repeated. After this time, the attenuation had increased but when filtered again through $0.22 \mu\text{m}$, the attenuation was the same than before. The spectrophotometric measurements done shortly after the additional filtration were always similar to PSICAM measurements, independent of the time when the PSICAM measurements were performed (Fig. 5). It is concluded that the sample should be filtered again through $0.22 \mu\text{m}$ filter shortly before measuring following the procedure described above. The increase in attenuation could be due to formation of larger particles after a storage of 4 to 24 h. As changes in absorption are not observed with the PSICAM measurements, the differences in the spectrophotometric measurements are probably due to purely scattering particles, because, as expected by theory, the PSICAM is not influenced by scattering. The additional filtration increases the reproducibility and, hence, accuracy of the spectrophotometric determination and reduces the error made by sample storage and handling.

All samples were taken from near the surface down to a depth of 200 m. Tables 1 and 2 show the absorption at 370 and 442 nm, and the exponential slope, S , of all surface samples measured with the photometer and the PSICAM together with the geographic position for each sample. The absorption at 442 nm (PSICAM data) ranged from 0.103 to 0.519 m^{-1} for samples from the North Sea (Table 1) and from 0.004 to 0.046 m^{-1} for samples from the Atlantic Ocean (Table 2). The slope (PSICAM data) ranged from 0.0147 to 0.0215 nm^{-1} . The slope for all samples from the North Sea was relatively constant (0.0166 to 0.0182 nm^{-1}), despite the fact that they were taken at different times of the year, had different salinities (25–31), and the absolute absorption value was varying strongly over a

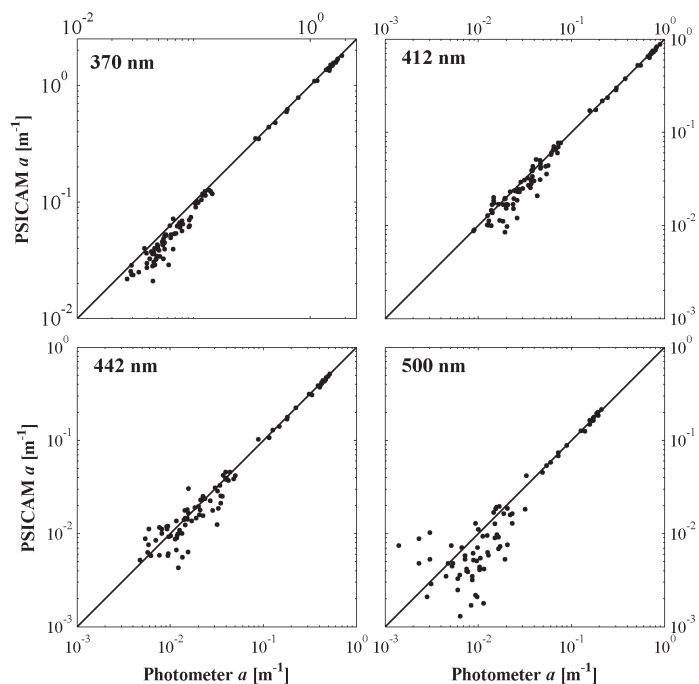


Fig. 7. Comparison between absorption coefficients measured with the PSICAM and with the spectrophotometer. Shown are the results at wavelengths of 370, 412, 442, and 500 nm on a log-log scale. The 1:1 correspondence is plotted in each panel. Note the different scales used for the 370 nm data.

short distance. Hence, the Atlantic sample showed a higher variability in slope.

Figure 6 shows a set of typical CDOM absorption spectra when determined with the two different instruments. The relative differences were small at higher absorption values (shorter wavelengths) and larger at lower values (longer wavelengths). At very low absorption ($< 0.005 \text{ m}^{-1}$) the photometric measurements were not reliable and showed an increased noise in the data (see Figures 6 and 7 at $> 500 \text{ nm}$). In general, the spectrophotometer data of the Atlantic samples had a high noise level and sometimes showed regular noise pattern which were induced by pitch and roll of the ship (see Fig. 6). Due to the concept of the PSICAM the noise was much lower and the ship's motion did not influence the absorption measurement.

At wavelengths $\leq 412 \text{ nm}$, the spectrophotometric measurements gave higher absorption coefficients than the PSICAM measurements (see Fig. 7). Figure 8 shows the difference in absorption coefficients between PSICAM and photometer at 370 and 442 nm when plotted against the absorption at 370 nm. There is a regular offset at 370 nm of around $+0.01 \text{ m}^{-1}$ with some higher values at higher absorption, whereas the differences at 442 nm are scattered around the zero line. These wavelength-dependent differences could be attributed to a remaining scattering error in the spectrophotometric setup, when scattering would increase with shorter wavelengths (typical for Rayleigh scattering). This limits the direct comparison between PSICAM and photometer to wavelengths $> 412 \text{ nm}$.

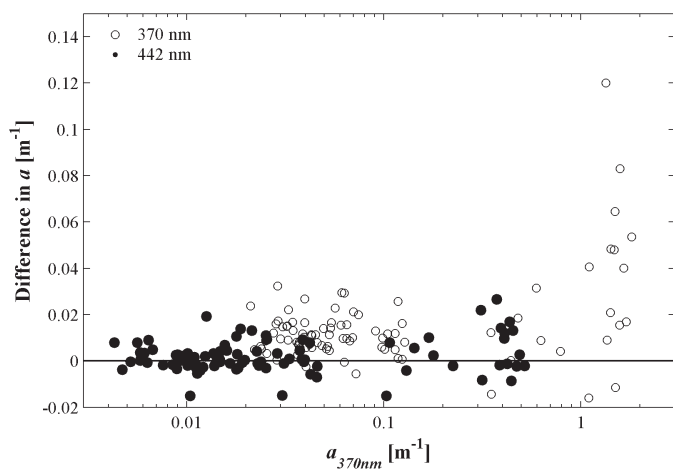


Fig. 8. Differences between absorption coefficients measured with the PSICAM and those measured with the spectrophotometer. Shown are absolute differences at 370 and 442 nm plotted as a function of absorption at 370 nm on a log scale.

The agreement at longer wavelengths (442 and 500 nm) was high, and the data are scattered around the 1:1 correspondence (Fig. 7). Considering the values at wavelengths > 412 nm, the PSICAM results were not different from that determined spectrophotometrically.

One parameter that is used to analyze CDOM absorption spectra is the exponential slope of the decreasing absorption with wavelength. Differences in slope are attributed to differences in the composition of CDOM (fulvic versus humic acid, Carder et al. 1989, Green and Blough 1994). A comparison of the slopes determined from absorption data of the two different instruments is shown in Fig. 9. The ratio of the two separately determined slopes is near 1.0 for samples of higher absorption, but deviated from 1.0 for sample with lower absorption. This is mainly due to the higher noise in the spectrophotometric data, when absorption is low. The sum of residuals obtained by the fitting procedure was one to two orders of magnitude higher for data of the spectrophotometer measurements than for that of the PSICAM measurements (data not shown).

Discussion

We conclude that the PSICAM provides exactly the same absorption values as determined with a spectrophotometer, but that the PSICAM is more sensitive and much less influenced by adverse scattering effects. The precision of the PSICAM determination was shown to be better than that of a typical spectrophotometer setup. The remaining differences in absorption at shorter wavelengths can be attributed to an adverse scattering influence on the spectrophotometric determination. This adverse influence cannot totally be precluded with filtration through $0.22 \mu\text{m}$ filters, either because of the influence of the remaining small particles, which by definition are then part of Gelbstoff, or because of a formation of

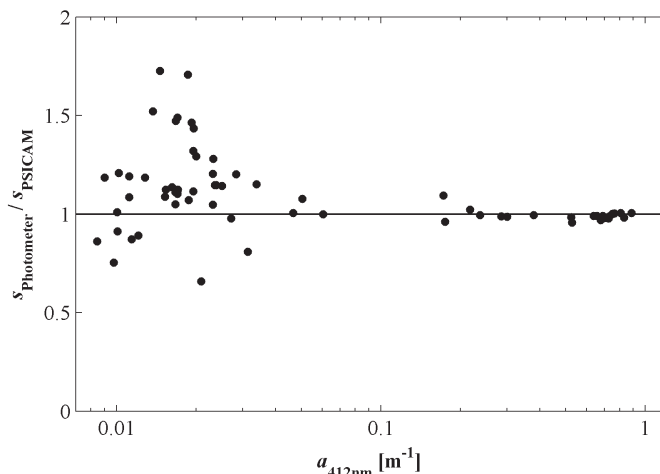


Fig. 9. Ratio between the exponential slope of the CDOM absorption, S , determined for absorption data measured by the spectrophotometer to that measured by the PSICAM ($S_{\text{photometer}}/S_{\text{PSICAM}}$). The data are plotted as a function of absorption at 412 nm.

new particles in the filtrate. In general, due to its much larger mean optical pathlength and the negligible scattering influence, the PSICAM is superior to the photometric setup in the determination of CDOM absorption coefficients. Especially at low absorption values, like in oligotrophic oceanic regions, and at longer wavelengths the absorption can accurately be determined with the PSICAM where the spectrophotometric setup failed, as the absorption is near or below the detection limit of photometric determinations. The low signal-to-noise ratio of the spectrophotometric determination also limits the accuracy of the determination of the exponential slope from photometric data in oligotrophic waters. The PSICAM as a rather simple instrument will, in future, improve our ability to perform accurate absorption measurement in oligotrophic water. Comparison with other types of instruments, like the Wetlabs-ACS or liquid waveguide systems should follow. Because of its simplicity, we expect that the instrument can be developed to work as an in situ profiling optical instrument, allowing CDOM and particulate absorption measurements over the whole water column.

References

- Blough, N. V., O. C. Zafiriou, and J. Bonilla. 1993. Optical absorption spectra of waters from the Orinoco River outflow: terrestrial input of coloured organic matter to the Caribbean. *J. Geophys. Res.* 98:2271-2278.
- Brando, V. E., J. T. O. Kirk, P. J. Daniel, K. Oubelkheir, A. G. Dekker, and L. Clementson. 2004. Measured sensitivity of the PSICAM: effects of anisotropic light source, fluorescence, temperature and salinity. In: *Proceedings of the Ocean Optics XVII Conference, Fremantle, October 25-29, 2002, Australia.*
- Bricaud, A., A. Morel, and L. Prieur. 1981. Absorption by dissolved organic matter of the sea (yellow substance) in the UV and visible domains. *Limnol. Oceanogr.* 26:43-53.

- Carder, K. L., R. G. Steward, G. R. Harvey, and P. B. Ortner. 1989. Marine humic and fulvic acids: Their effects on remote sensing of ocean chlorophyll. *Limnol. Oceanogr.* 34:68-81.
- D'Sa, E. J., R. G. Steward, A. Vodacek, N. V. Blough, and D. Phinney. 1999. Determining optical absorption of colored dissolved organic matter in seawater with a liquid capillary waveguide. *Limnol. Oceanogr.* 44:1142-1148.
- Green, S. A., and N. V. Blough. 1994. Optical absorption and fluorescence properties of chromophoric dissolved organic matter in natural waters. *Limnol. Oceanogr.* 39:1903-1916.
- Hansell, D., and C. Carlson. 2002. Biogeochemistry of marine dissolved organic matter. Academic Press.
- Kalle, K. 1949. Fluorescence and gelbstoff in the Gulf of Bothnia and Finland. *Dtsch. Hydrogr. Z.* 2:117-124.
- Kirk, J. T. O. 1997. Point-source integrating-cavity absorption meter: theoretical principles and numerical modeling. *Appl. Opt.* 36:6123-6128.
- Langford, V. S., A. J. McKinley, and T. I. Quickenden. 2001. Temperature dependence of the visible-near-infrared absorption spectrum of liquid water. *J. Phys. Chem. A* 105: 8916-8921.
- Leathers, R. A., T. V. Downes, and C. O. Davis. 2000. Analysis of a point-source integrating-cavity absorption meter. *Appl. Opt.* 39:6118-6127.
- Miller, R. L., M. Belz, and S. Y. Liu. 2000. Measuring the absorption of CDOM in the field using a multiple path-length liquid waveguide system. In: Proceedings of the Ocean Optics XV conference, Monaco, 16-20 October 2000.
- , ———, C. Del Castillo, and R. Trzaska. 2002. Determining CDOM absorption spectra in diverse coastal environments using a multiple pathlength, liquid core waveguide system. *Cont. Shelf Res.* 22:1301-1310.
- Pegau, W. S., D. Gray, and J. R. V. Zaneveld. 1997. Absorption and attenuation of visible and near-infrared light in water: dependence on temperature and salinity. *Appl. Opt.* 36: 6035-6046.
- Pope, R. M., A. D. Weidemann, and E. S. Fry. 2000. Integrating cavity absorption meter measurements of dissolved substances and suspended particles in ocean water. *Dyn. Atmos. Oceans* 31:307-320.
- Röttgers, R., W. Schönfeld, P. -R. Kipp, and R. Doerffer. 2005. Practical test of a point-source integrating cavity absorption meter: the performance of different collector assemblies. *Appl. Opt.* 44:5549-5560.
- Sullivan, J. M., M. S. Twardowski, J. R. V. Zaneveld, C. M. Moore, A. H. Barnard, P. L. Donaghay, and B. Rhoades. 2006. The hyperspectral temperature and salt dependencies of absorption by water and heavy water in the 400–750 nm spectral range. *Appl. Opt.* 45:5294-5309.
- Tilstone, G., and others. 2002. REVAMP, Regional Validation of MERIS Chlorophyll products in North Sea coastal waters. REVAMP Protocols, Protocols document, EU, EVG1-CT-2001-00049, 77p.

Submitted 9 March 2006

Revised 19 January 2007

Accepted 29 January 2007